

1 Exogenous phosphatidic acid reduces acetaminophen-induced liver  
2 injury in mice by activating the interleukin-6 – Hsp70 axis through inter-  
3 organ crosstalk

4 Melissa M. Clemens<sup>a,b,\*</sup>, Stefanie Kennon-McGill<sup>c</sup>, Joel H. Vazquez<sup>a,b</sup>, Owen W. Stephens<sup>d</sup>,  
5 Erich A. Peterson<sup>d</sup>, Donald J. Johann<sup>d</sup>, Felicia D. Allard<sup>e</sup>, Eric U. Yee<sup>e</sup>, Sandra S. McCullough<sup>f</sup>,  
6 Laura P. James<sup>f</sup>, Brian N. Finck<sup>g</sup>, Mitchell R. McGill<sup>a,c,h,#</sup>

7 <sup>a</sup>Dept. of Pharmacology and Toxicology, College of Medicine, University of Arkansas for  
8 Medical Sciences, 4301 W. Markham St., Little Rock, AR, 72205 USA

9 <sup>b</sup>Interdisciplinary Graduate Program in Biomedical Sciences, Graduate School, University of  
10 Arkansas for Medical Sciences, 4301 W. Markham St., Little Rock, AR, 72205 USA

11 <sup>c</sup>Dept. of Environmental and Occupational Health, Fay W. Boozman College of Public Health,  
12 University of Arkansas for Medical Sciences, 4301 W. Markham St., Little Rock, AR, 72205  
13 USA

14 <sup>d</sup>Winthrop P. Rockefeller Cancer Institute, University of Arkansas for Medical Sciences, 4301  
15 W. Markham St., Little Rock, AR, 72205 USA

16 <sup>e</sup>Dept. of Pathology, Renaissance School of Medicine, Stony Brook University, 101 Nicolls Rd.,  
17 Stony Brook, NY, 11794 USA

18 <sup>f</sup>Dept of Pediatrics, College of Medicine, University of Arkansas for Medical Sciences, 4301 W.  
19 Markham St., Little Rock, AR, 72205 USA

20 <sup>g</sup>Div. of Geriatrics and Nutritional Sciences, Dept. of Internal Medicine, Washington University  
21 School of Medicine, 660 S. Euclid Ave., St. Louis, MO, 63110 USA

22 <sup>h</sup>Center for Dietary Supplement Research, University of Arkansas for Medical Sciences, 4301  
23 W. Markham St., Little Rock, AR, 72205 USA

24

25 \*Melissa M. Clemens unexpectedly passed away on May 24<sup>th</sup>, 2020, after writing the first draft  
26 of this manuscript. The corresponding author assumes responsibility for all changes made after  
27 her death.

28

29 <sup>#</sup>To whom correspondence should be addressed ([mmcgill@uams.edu](mailto:mmcgill@uams.edu))

30

31 **Abbreviations**

32 APAP, acetaminophen; ALF, acute liver failure; NAPQI, N-acetyl-p-benzoquinone imine; JNK,  
33 c-Jun N-terminal kinase; NAC, N-acetylcysteine; PA, phosphatidic acid; IL-6, interleukin-6;  
34 ALT, alanine aminotransferase; GSH, reduced glutathione; GSSG, oxidized glutathione; GSK3 $\beta$ ,  
35 glycogen synthase kinase 3 $\beta$ ; GO:BP, gene ontology:biological processes; Stat3, signal  
36 transducer and activator of transcription 3; KC, Kupffer cell; eWAT, epididymal white adipose  
37 tissue; PcnA, proliferating cell nuclear antigen; Hif2 $\alpha$ , hypoxia-inducible factor; CCl<sub>4</sub>, carbon  
38 tetrachloride; mTORC1, mechanistic target of rapamycin complex 1; LysoPA, lyso-phosphatidic  
39 acid; DAG, diacylglycerol.

40

41 **Abstract**

42 We previously demonstrated that endogenous phosphatidic acid (PA) promotes liver  
43 regeneration after acetaminophen (APAP) hepatotoxicity in mice. Based on that, we  
44 hypothesized that exogenous PA is also beneficial. To test that, we treated mice with a toxic  
45 APAP dose at 0 h, followed by PA or vehicle at multiple timepoints. We then collected blood  
46 and liver at 6, 24, and 52 h. Post-treatment with PA protected against liver injury at 6 h, and the  
47 combination of PA and N-acetyl-cysteine (NAC) further reduced injury compared to NAC alone.  
48 Interestingly, PA had no effect on major early mechanisms of APAP toxicity, including APAP  
49 bioactivation, oxidative stress, JNK activation, and mitochondrial damage. However,  
50 transcriptomics revealed that PA activated interleukin-6 (IL-6) signaling in the liver, and IL-6  
51 was increased in serum from PA-treated mice. Furthermore, PA did not protect against APAP in  
52 IL-6-deficient mice. Additional experiments revealed that PA induced heat shock protein 70  
53 (Hsp70) in the liver in WT mice but not in IL-6 KO mice. Furthermore, IL-6 expression  
54 increased 18-fold in adipose tissue after PA, indicating that adipose tissue is a likely source of  
55 the increased IL-6 due to PA treatment. Surprisingly, however, exogenous PA did not alter  
56 regeneration, despite the widely accepted role of IL-6 in liver repair. These data reinforce the  
57 protective role of IL-6 and Hsp70 in APAP hepatotoxicity, provide new insight into the role of  
58 IL-6 in liver regeneration, and indicate that exogenous PA or PA derivatives may one day be a  
59 useful adjunct treatment for APAP overdose with NAC.

60

61

62

## 63 1. Introduction

64 Acetaminophen (APAP) is a popular analgesic and antipyretic drug (Kaufman et al.,  
65 2002), but overdose causes severe acute liver injury. It is currently the leading cause of acute  
66 liver failure (ALF) throughout much of the world (Lee, 2008). Conversion of APAP to the  
67 reactive metabolite N-acetyl-*p*-benzo quinoneimine (NAPQI) initiates the hepatotoxicity.  
68 NAPQI binds to free sulfhydryl groups on amino acid residues, depleting hepatic glutathione and  
69 damaging proteins (Jollow et al., 1973; Mitchell et al., 1973; McGill and Hinson, 2020). The  
70 protein binding leads to mitochondrial dysfunction and oxidative stress (Jaeschke, 1990; Cover  
71 et al., 2005), which activates the c-Jun N-terminal kinases 1/2 (JNK) and other kinases  
72 (Gunawan et al., 2006; Hanawa et al., 2008; Nakagawa et al., 2008; Ramachandran et al., 2013).  
73 Activated JNK translocates from the cytosol to mitochondria, where it exacerbates the  
74 mitochondrial dysfunction by reducing mitochondrial respiration (Hanawa et al., 2008; Win et  
75 al., 2016). Eventually, the mitochondrial permeability transition occurs (Kon et al., 2004; Reid et  
76 al., 2005), and the mitochondrial damage causes release of endonucleases from mitochondria,  
77 which then cleave nuclear DNA (Bajt et al., 2006). The affected hepatocytes die by necrosis  
78 (Gujral et al., 2002; McGill et al., 2011; 2012).

79 Phosphatidic acid (PA) is a critically important lipid in all prokaryotic and eukaryotic  
80 cells. It is the simplest diacylated glycerophospholipid, having a bare phosphate head group. In  
81 cell and organelle membranes, the small size and negative charge of the head group likely  
82 promotes negative curvature that may be important for membrane fission (Kooijman et al.,  
83 2003). It is also a major metabolic intermediate, serving as a key precursor for synthesis of all  
84 other phospholipids as well as triglycerides (Pokotyła et al., 2018). Finally, it is a major lipid  
85 second messenger that is known to play a role in nutrient sensing and cell proliferation via

86 mechanistic target of rapamycin (mTOR) signaling (Fang et al., 2001; Foster, 2013; Pokotyla et  
87 al., 2018).

88 We recently demonstrated that phosphatidic acid (PA) is beneficial after APAP-induced  
89 liver injury in mice through an entirely novel mechanism (Lutkewitte et al., 2018; Clemens et al.,  
90 2019a). Briefly, we found that *endogenous* PA is elevated in the liver after APAP overdose, and  
91 that it promotes cell proliferation and therefore liver repair by regulating glycogen synthase  
92 kinase 3 $\beta$  (GSK3 $\beta$ ) (Lutkewitte et al., 2018; Clemens et al., 2019). However, we did not test the  
93 effect of *exogenous* administration of PA on APAP-induced liver injury. In the present study, we  
94 hypothesized that exogenous PA is beneficial in a mouse model of APAP overdose. Our data  
95 demonstrate that it reduces APAP hepatotoxicity by increasing systemic interleukin-6 (IL-6)  
96 from adipose tissue, which in turn upregulates expression of protective Hsp70 in the liver.

97

## 98 **2. Experimental procedures**

### 99 **2.1. Animals.**

100 Male wild-type (WT) C57BL/6J mice and IL-6 knockout mice (IL-6 KO; B6.129S2-  
101 Il6<sup>tm1Kopf/J</sup>) between the ages of 8 and 12 weeks were obtained from The Jackson Laboratory  
102 (Bar Harbor, ME, USA). The mice were housed in a temperature-controlled 12 h light/dark cycle  
103 room and allowed free access to food and water. The APAP and PA solutions were prepared  
104 fresh on the morning of each experiment. APAP was prepared by dissolving 15 mg/mL APAP  
105 (Sigma, St. Louis, MO, USA) in 1x PBS with gentle heating and intermittent vortexing. The PA  
106 solution was prepared by re-constituting purified egg PA extract (Avanti Polar Lipids, Alabaster,  
107 AL, USA) at 10 mg/mL in 10% DMSO in 1x PBS, warming to 80°C for 20-30 min with

108 intermittent mixing to obtain a uniform hazy suspension, and cooling to room temperature  
109 immediately before injection. To determine if PA affects liver injury, WT mice (n = 5-10 per  
110 group) were fasted overnight then injected (i.p.) with 250 mg/kg APAP at 0 h, followed by 10%  
111 DMSO vehicle (Veh) or 20 mg/kg PA (i.p.) at 2 h. Blood and liver tissue were collected at 6 h.  
112 We chose the 20 mg/kg dose of PA because it is commonly recommended when taken as a  
113 dietary supplement in humans. To determine if the combination of N-acetylcysteine (NAC) and  
114 PA reduces injury compared to NAC alone, some mice were injected with APAP at 0 h followed  
115 by 300 mg/kg NAC (dissolved in 1x PBS) and either PA or vehicle at 2 h (n = 7 per group).  
116 Blood was collected at 6 h. We chose the 300 mg/kg dose of NAC because it is approximately 2-  
117 fold greater than the typical loading dose in humans after APAP overdose. Using this high dose  
118 of NAC ensures that our results comparing NAC with APAP+NAC are conservative and robust.  
119 For transcriptomics, the original PA experiment was repeated at the 6 h time point with addition  
120 of a vehicle-only control group (n = 5 per group). To determine if PA protection depends upon  
121 IL-6, the experiment was repeated again at the 6 h time point using IL-6 KO mice (n = 5-6 per  
122 group) and a similar but higher dose of APAP (350 mg/kg). The change in APAP dose in the  
123 latter experiment was due to an adjustment made to our university animal use protocol during the  
124 course of the study and unrelated to our data from these experiments. Finally, to test the role of  
125 Kupffer cells, the original PA experiment was repeated at the 6 h time point with WT mice (n =  
126 10 per group) after 24 h i.v. (tail vein) pre-treatment with 0.2 mL of 17 mM liposomal clodronate  
127 (Clodrosome, Brentwood, TN, USA). All study protocols were approved by the Institutional  
128 Animal Care and Use Committee of the University of Arkansas for Medical Sciences.

## 129 **2.2. Subcellular fractionation**

130 Right and caudate liver lobes were homogenized in ice cold isolation buffer containing  
131 220 mM mannitol, 70 mM sucrose, 2.5 mM HEPES, 10 mM EDTA, 1mM ethylene glycol tetra-  
132 acetic acid and 0.1% bovine serum albumin (pH 7.4) using a Thermo-Fisher Bead Mill.  
133 Subcellular fractions were obtained by differential centrifugation. Samples were centrifuged at  
134 2,500 x g for 10 min to blood cells and debris. Supernatants were then centrifuged at 20,000 x g  
135 for 10 min to pellet mitochondria. The supernatant was retained as the cytosol fraction. Pellets  
136 containing mitochondria were then resuspended in 100  $\mu$ L of isolation buffer and freeze-thawed  
137 three times using liquid nitrogen to disrupt the mitochondrial membranes. Protein concentration  
138 was measured in both the mitochondrial and cytosol fractions using the BCA assay, and the  
139 samples were used for western blotting as described below.

### 140 **2.3. Clinical Chemistry**

141 Alanine aminotransferase (ALT) was measured in serum using a kit from Point Scientific  
142 Inc. (Canton, MI, USA) according to the manufacturer's instructions.

### 143 **2.4. Histology**

144 Liver tissue sections were fixed in 10% formalin. For hematoxylin & eosin (H&E)  
145 staining, fixed tissues were embedded in paraffin wax, then 5  $\mu$ m sections were mounted on  
146 glass slides and stained according to a standard protocol. Necrosis was quantified in the H&E-  
147 stained sections by two independent, fellowship-trained, hepatobiliary pathologists who were  
148 both blinded to sample identity. Percent necrosis was then averaged for each animal. For Oil  
149 Red O staining, fixed tissues were embedded in OCT compound and rapidly frozen by placing  
150 on a metal dish floating in liquid nitrogen. 8  $\mu$ m sections were cut and mounted on positively-  
151 charged glass slides. The sections were allowed to dry for 30 min at room temperature, then

152 treated with 60% isopropanol for 5 min, followed by freshly prepared Oil Red O solution in  
153 isopropanol for 10 min, and then 60% isopropanol for an additional 2 min. The sections were  
154 then rinsed with PBS, treated with Richard-Allan Gill 2 hematoxylin solution (Thermo Fisher,  
155 Waltham, MA, USA) for 1 min, and rinsed again with PBS before cover-slipping. Digital  
156 images were taken using a Labomed Lx400 microscope with digital camera (Labo American  
157 Inc., Fremont, CA, USA).

## 158 **2.5. Western Blotting**

159 Liver tissues were homogenized in 25 mM HEPES buffer with 5 mM EDTA, 0.1%  
160 CHAPS, and protease inhibitors (pH 7.4). Protein concentration was measured using a  
161 bicinchoninic acid (BCA) assay. The samples were then diluted in homogenization buffer, mixed  
162 with reduced Laemmli buffer, and boiled for 1 min. Equal amounts (60 µg protein) were added  
163 to each lane of a 4-20% Tris-glycine gel. After electrophoresis, proteins were transferred to  
164 PVDF membranes and blocked with 5% milk in Tris-buffered saline with 0.1% Tween 20.  
165 Primary monoclonal antibodies were purchased from Cell Signaling Technology (Danvers, MA,  
166 USA): p-JNK (Cat. No. 4668), JNK (Cat. No. 9252), AIF (Cat. No. 5318), Cytochrome-C (Cat.  
167 No.11940), AIF (Cat. No. 5318), GSK3β (Cat. No. 9315), phospho-GSK3β (Cat. No. 9323), and  
168 β-actin (Cat. No. 4967). All primary antibodies were used at 1:1000 dilution. Secondary  
169 antibodies were purchased from LiCor Biosciences (Lincoln, NE, USA): IRDye 680 goat anti-  
170 mouse IgG (Cat. No. 926-68070) and IRDye 800CW goat anti-rabbit IgG (Cat. No. 926-32211).  
171 All secondary antibodies were used at 1:10,000 dilution. Bands were visualized using the  
172 Odyssey Imaging System (LiCor Biosciences, Lincoln, NE, USA).

## 173 **2.6. Glutathione measurement**



174 Total glutathione (GSH+GSSG) and oxidized glutathione (GSSG) were measured using a  
175 modified Tietze assay, as we previously described in detail (McGill and Jaeschke, 2015).

### 176 **2.7. APAP-protein adduct measurement**

177 APAP-protein adducts were measured using high pressure liquid chromatography  
178 (HPLC) with electrochemical detection, as previously described (Muldrew et al., 2002; McGill et  
179 al., 2013).

### 180 **2.8. Transcriptomics**

181 The Supporting Information section contains all details concerning RNA-seq sample  
182 prep, next generation sequencing, and bioinformatic analyses.

### 183 **2.9. Statistics**

184 Normality was assessed using the Shapiro-Wilk test. Normally distributed data were  
185 analyzed using a t-test for comparison of two groups or one-way ANOVA with post-hoc  
186 Student-Neuman-Keul's for comparison of three or more groups. Data that were not normally  
187 distributed were analyzed using a nonparametric Mann-Whitney U test for comparison of two  
188 groups, or one-way ANOVA on ranks with post-hoc Dunnet's test to compare three or more. All  
189 statistical tests were performed using SigmaPlot 12.5 software (Systat, San Jose, CA, USA).

190

## 191 **3. Results**

### 192 **3.1. Exogenous PA reduces liver injury at 6 h after APAP overdose.**

193 To determine the effect of exogenous PA treatment on APAP-induced liver injury, we  
194 treated mice with APAP at 0 h followed by PA or vehicle at 2 h. We then collected blood and

195 liver tissue at 6 h. We observed a significant reduction in serum ALT values in the PA-treated  
196 mice at 6 h post-APAP (Fig. 1A). Two blinded, fellowship-trained hepatobiliary and GI  
197 pathologists independently confirmed the reduction in injury based on histology (Fig. 1B and  
198 Table 1). NAC is the current standard-of-care treatment for APAP-induced liver injury in  
199 patients. To determine if the combination of PA and NAC can further reduce injury after APAP  
200 overdose compared to the standard-of-care alone, we treated mice with APAP followed by 300  
201 mg/kg NAC and either vehicle or PA. The combination of NAC plus PA significantly decreased  
202 serum ALT compared to NAC plus vehicle (Table 2). Together, these data demonstrate that  
203 exogenous PA can reduce liver APAP-induced liver injury and indicate that it could be useful as  
204 an adjunct treatment for APAP overdose.

### 205 ***3.2. Exogenous PA does not affect the canonical mechanisms of APAP-induced liver*** 206 ***injury.***

207 Next, we sought to determine the mechanisms by which exogenous PA reduces early  
208 APAP hepatotoxicity. The initiating step in APAP-induced liver injury is formation of the  
209 reactive metabolite N-acetyl-*p*-benzoquinone imine (NAPQI), which depletes glutathione and  
210 binds to proteins. To determine if the decrease in liver injury at 6 h was due to an effect on  
211 NAPQI formation, we measured total glutathione (GSH + GSSG) and APAP-protein adducts in  
212 the liver. We did not detect a significant difference between the APAP plus vehicle and APAP  
213 plus PA groups in either parameter (Fig. 2A,B).

214 To determine if PA protects by preventing the early mitochondrial dysfunction and  
215 oxidative stress after APAP overdose, we measured GSSG in the liver. There was no significant  
216 difference in either total GSSG or the percentage of glutathione in the form of GSSG (%GSSG)  
217 between the two groups (Fig. 2C,D). To test if JNK activation and/or mitochondrial translocation

218 were affected, we immunoblotted for phosphorylated and total JNK. Again, we could not detect  
219 a difference between the groups (Fig. 2E,F). To determine if PA had an effect on mitochondrial  
220 damage downstream of JNK, and therefore mitochondrial rupture, we also immunoblotted for  
221 AIF and cytochrome c in cytosolic fractions, and again no differences were detected (Fig. 2G).  
222 Because we previously found that endogenous PA can regulate GSK3 $\beta$  activity through Ser9  
223 phosphorylation (Clemens et al., 2019a) and because active GSK3 $\beta$  is known to exacerbate  
224 APAP-induced liver injury (Shinohara et al., 2010), we also measured GSK3 $\beta$  Ser9  
225 phosphorylation but once again observed no differences (Fig. 2H). Finally, as an additional  
226 indicator of mitochondrial function, we performed Oil Red O staining of triglycerides in frozen  
227 liver sections to assess lipid oxidation. Consistent with previous studies (Bhattacharyya et al.,  
228 2014; Borude et al., 2018), we observed Oil Red O accumulation in the damaged hepatocytes  
229 within centrilobular regions, indicating loss of  $\beta$ -oxidation due to mitochondrial damage, but  
230 again we saw no apparent difference between the groups (Fig. 2I). Altogether, these data largely  
231 rule out an effect of PA on APAP bioactivation, oxidative stress, and overt mitochondrial  
232 damage.

### 233 **3.3. Exogenous PA protects through IL-6 signaling in the liver.**

234 To identify other mechanisms by which PA might reduce early APAP hepatotoxicity, we  
235 performed next generation RNA sequencing in liver tissue from mice treated with vehicle only,  
236 APAP plus vehicle, and APAP plus PA. We found that 6,192 genes were differentially expressed  
237 between the vehicle only and the APAP plus vehicle groups. Consistent with the protein  
238 alkylation, oxidative stress, and inflammation known to occur in APAP hepatotoxicity, gene  
239 ontology (biological processes; GO:BP) analysis revealed that genes involved in protein  
240 refolding, cell responses to chemical stimulus, and toll-like receptor signaling were increased by

241 APAP, while various cell growth and cell signaling processes were decreased (Fig. 3A). 388  
242 genes were differentially expressed between the APAP plus vehicle and APAP plus PA groups.  
243 This was insufficient for complete GO analysis, but it is notable that the GO:BP term “acute  
244 inflammatory response” was over-represented in the APAP plus PA group when using a log<sub>2</sub>  
245 fold-change threshold of 1. Furthermore, hierarchical clustering analysis (Fig. 3B) showed clear  
246 separation of the APAP plus vehicle and APAP plus PA groups across the five biological  
247 replicates per group. Importantly, upstream analysis (Ingenuity Pathway Analysis [IPA])  
248 revealed activation of signaling downstream of IL-6 and its target transcription factor signal  
249 transducer and activator of transcription 3 (Stat3) (Table 3). Recent studies have demonstrated  
250 that IL-6 is protective in APAP hepatotoxicity (Gao et al., 2019), and it was previously  
251 demonstrated that treatment with exogenous PA at doses similar to those we used here rapidly  
252 increase serum IL-6 concentration (Lim et al., 2003). Thus, to confirm that PA increased serum  
253 IL-6 in our experiment, we measured IL-6 protein in serum at 6 h post-APAP. Importantly, IL-6  
254 was significantly elevated in the APAP plus PA mice compared to the APAP plus vehicle  
255 animals (Fig. 3C). Together, these data indicate that PA may protect against APAP toxicity by  
256 activating IL-6.

257 To confirm that exogenous PA affects APAP-induced liver injury through IL-6, we  
258 compared the effect of exogenously administered PA on APAP hepatotoxicity in WT and IL-6  
259 KO mice at 6 h post-APAP. Importantly, PA did not reduce liver injury in the KO mice, despite  
260 protecting in the WT mice in the same experiment (Fig. 4). In fact, it appeared to worsen injury  
261 in the IL-6 KO mice. These data clearly demonstrate that IL-6 is necessary for the protection  
262 provided by exogenous PA in WT mice, and support previous work indicating that IL-6 is  
263 protective in APAP-induced liver injury overall.

264 It is known that IL-6 increases expression of Hsp70 and other heat shock proteins in the  
265 liver during APAP hepatotoxicity (Masubuchi et al., 2003). Furthermore, Hsp70 is protective  
266 after APAP overdose (Tolson et al., 2006). These data suggest that PA might protect through IL-  
267 6-mediated induction of Hsp70. To test that, we immunoblotted for Hsp70 in liver tissue from  
268 the WT and IL-6 KO mice. Importantly, Hsp70 protein level was significantly increased by  
269 exogenous PA in the WT mice but not the KO mice (Fig. 5), indicating that PA may indeed  
270 protect through an Hsp70 – IL-6 axis.

#### 271 ***3.4. Adipose tissue is a likely source of increased IL-6 after PA treatment.***

272 Multiple liver cell types express IL-6, but Kupffer cells (KCs) are the major producers.  
273 To determine if the increase in IL-6 caused by treatment with exogenous PA is due to increased  
274 expression of IL-6 in KCs or other liver cells, we measured IL-6 mRNA in liver tissue in the  
275 APAP plus vehicle and APAP plus PA groups. We could not detect a significant difference in  
276 IL-6 expression between the two groups (Fig. 6A). Because KCs account for only a small portion  
277 of cells in the liver, it is possible that total liver mRNA has poor sensitivity to detect changes  
278 specifically within KCs. Thus, to further test if KCs are the source of IL-6 after PA treatment, we  
279 pre-treated mice with liposomal clodronate to ablate macrophages. The following day, we  
280 administered APAP followed by either PA or vehicle. Blood and liver tissue were collected at 6  
281 h post-APAP. Surprisingly, serum ALT was still significantly reduced by PA (Fig. 6B), despite  
282 depletion of the liver macrophages (Fig. 6C). These data indicate that the liver itself is probably  
283 not the major source of IL-6 after PA treatment.

284 To identify other possible sources of IL-6, we treated mice with PA or vehicle and  
285 collected liver, kidney, lung, epididymal white adipose tissue (eWAT), and spleen 4 h later. We  
286 chose these tissues because they have high basal IL-6 expression and are known to produce IL-6

287 in other disease contexts. Interestingly, we observed an 18-fold increase in IL-6 mRNA in eWAT  
288 (Fig. 6D). We could not detect differences in the other tissues. These data reveal that adipose  
289 tissue is a likely source of increased systemic IL-6 after PA treatment, indicating inter-organ  
290 crosstalk between liver and fat.

### 291 **3.5. Exogenous PA does not promote liver regeneration.**

292 Finally, because we previously demonstrated that endogenous PA promotes liver  
293 regeneration (Lutkewitte et al., 2018; Clemens et al., 2019a) and because IL-6 is a well-known  
294 driver of regeneration (Clemens et al., 2019b), we wanted to determine if exogenous PA  
295 enhances regeneration and repair after APAP overdose. To test that, we treated mice with APAP  
296 at 0 h, followed by exogenous PA or vehicle at 6, 24, and 48 h post-APAP. We selected these  
297 late post-treatment time points to avoid an effect on the early injury, which would have  
298 decreased liver regeneration secondary to the reduced injury. We then collected blood and liver  
299 tissue at 24 and 52 h. Although serum ALT was significantly decreased at 52 h (Fig. 7A), there  
300 was no apparent difference in area of necrosis (Fig. 7B) and no change in PcnA (Fig. 7C)  
301 between the treatment groups at either time point. These data indicate that exogenous PA, unlike  
302 endogenous PA, does not affect liver regeneration after APAP overdose.

303

## 304 **4. Discussion**

305 Together with our earlier work, the results from this study reveal that endogenous and  
306 exogenous PA have different beneficial effects in APAP hepatotoxicity involving different  
307 mechanisms of action. We previously demonstrated that endogenous PA accumulates in liver  
308 tissue and plasma after APAP overdose in both mice and humans (Lutkewitte et al., 2018).

309 Importantly, inhibition of the PA accumulation had no effect on injury in the mice, but did  
310 reduce regeneration and survival by de-regulating GSK3 $\beta$  activity through an effect on Ser9  
311 phosphorylation (Lutkewitte et al., 2018; Clemens et al., 2019a). In the present study, we found  
312 that exogenous PA reduces the early injury by increasing systemic IL-6 levels, but has no effect  
313 on GSK3 $\beta$  phosphorylation or liver regeneration. These data indicate that exogenous PA or PA  
314 derivatives may be a useful adjunct with NAC to treat early APAP hepatotoxicity in patients, but  
315 targeting PA-mediated signaling to promote liver regeneration in late presenters will require a  
316 different approach.

317 Our data demonstrate that exogenous PA reduced early injury but had no effect on the  
318 major intracellular mechanisms of APAP hepatotoxicity (NAPQI formation, oxidative stress,  
319 mitochondrial damage). Transcriptomics analysis then indicated that PA activated IL-6 signaling.  
320 Through upstream analysis, we observed activation of IL-6/STAT3 signaling in liver tissue from  
321 our PA-treated animals. We then demonstrated that PA does not protect in IL-6 KO mice. Those  
322 results are consistent with earlier data demonstrating that systemic administration of exogenous  
323 PA dramatically increases circulating levels of IL-6 (Lim et al., 2003). They also confirm the  
324 protective role of IL-6 in APAP hepatotoxicity. Masubuchi et al. (2003) reported that IL-6 KO  
325 mice have worse injury after APAP overdose. More recently, Gao et al. (2019) observed that  
326 administration of exogenous IL-6 is protective. Importantly, the protective effect of IL-6 likely  
327 involves heat shock proteins, since Hsp70 and others are increased in liver tissue after APAP  
328 treatment in an IL-6-dependent manner (Masubuchi et al., 2003) and Hsp70 KO worsens APAP  
329 toxicity (Tolson et al., 2006). Taken together with our data, it seems likely that exogenous PA  
330 delays injury through its effects on the IL-6-Hsp70 signaling axis.

331 Bae et al. (2017) recently demonstrated that exogenously administered lysoPA also  
332 protects against APAP hepatotoxicity. PA can be converted to lysoPA by phospholipases, so it is  
333 theoretically possible that lysoPA contributed to the protection we observed in our study.  
334 However, their data demonstrated that lysoPA protected by 1) preventing early glutathione  
335 depletion and increasing glutathione re-synthesis at 6 h post-APAP and by 2) altering JNK and  
336 GSK3 $\beta$  activation (Bae et al., 2017), while we could not detect any effect of exogenous PA on  
337 either glutathione or kinases in our experiments. These data indicate that PA protected through  
338 entirely different mechanisms in our study. However, Bae et al. (2017) also used a 1 h pre-  
339 treatment in most of their experiments, which has limited clinical relevance and makes it difficult  
340 to directly compare our results.

341 It is surprising that exogenous PA did not enhance liver regeneration after APAP  
342 overdose despite multiple treatments, especially considering the importance of IL-6 in liver  
343 repair. IL-6-deficient animals have delayed regeneration after partial hepatectomy, APAP  
344 overdose, and CCl<sub>4</sub> hepatotoxicity (Cressman et al., 1996; Selzner et al., 1999; James et al.,  
345 2003; Rio et al., 2008). On the other hand, Bajt et al. (2003) found that injection of recombinant  
346 IL-6 does not enhance regeneration after APAP overdose, and many treatments that do enhance  
347 regeneration do not increase IL-6. It may be the case then that basal IL-6 levels are sufficient to  
348 aid liver repair, such that reducing IL-6 can blunt regeneration but increasing it has no effect. In  
349 any case, IL-6 can clearly influence both early injury and later regeneration in multiple liver  
350 disease models, and we need more data to understand the details of those effects.

351

## 352 5. Conclusions



353 Overall, we conclude that post-treatment with exogenous PA likely reduces APAP  
354 hepatotoxicity in mice by increasing systemic IL-6, which then induces Hsp70 in the liver.  
355 Because PA is readily available over-the-counter as a supplement due to its purported ergogenic  
356 effects (Shad et al., 2015) and because the combination of PA and NAC protected better than  
357 NAC alone in our experiments, exogenous PA or PA derivatives may one day be a useful adjunct  
358 with NAC for treatment of early-presenting APAP overdose patients. However, more research is  
359 needed to test that possibility. In future studies, we will optimize the dose of PA for protection,  
360 test additional treatment regimens and time points, and explore the effects of different acyl  
361 chains. We will also test the effects of both endogenous and exogenous PA in other liver disease  
362 models.

363

#### 364 **Acknowledgements**

365 This study was funded in part by a Pinnacle Research Award from the AASLD Foundation  
366 (MRM), and National Institutes of Health grants T32 GM106999 (MMC and JHV), R01  
367 DK104735 (BFN), R01 DK117657 (BFN), R42 DK121652 (BFN), R56 DK111735 (BFN), R42  
368 DK079387 (LPJ), and UL1 TR003107 (LPJ, SKM) and TR003108 (LPJ, SKM). We are grateful  
369 for expert technical assistance provided by the Dept. of Laboratory Animal Medicine at UAMS  
370 (especially Robin Mulkey) and by the Experimental Pathology Core (especially Jennifer D.  
371 James, HT(ASCP), HTL, QIHC).

372

373 **References**

- 374 Bae GH, Lee SK, Kim HS, Lee M, Lee HY, Bae YS. 2017. Lysophosphatidic acid protects  
375 against acetaminophen-induced acute liver injury. *Exp. Mol. Med.* 49, e407.
- 376 Bajt ML, Cover C, Lemasters JJ, Jaeschke H. 2006. Nuclear translocation of endonuclease G and  
377 apoptosis-inducing factor during acetaminophen-induced liver cell injury. *Toxicol. Sci.*  
378 94, 217–225.
- 379 Bajt ML, Knight TR, Farhood A, Jaeschke H. 2003. Scavenging peroxynitrite with glutathione  
380 promotes regeneration and enhances survival during acetaminophen-induced liver injury  
381 in mice. *J. Pharmacol. Exp. Ther.* 307, 67–73.
- 382 Bhattacharyya S, Yan K, Pence L, Simpson PM, Gill P, Letzig LG, et al. 2014. Targeted liquid  
383 chromatography-mass spectrometry analysis of serum acylcarnitines in acetaminophen  
384 toxicity in children. *Biomark. Med.* 8, 147–159.
- 385 Borude P, Bhushan B, Gunewardena S, Akakpo J, Jaeschke H, Apte U. 2018. Pleiotropic Role of  
386 p53 in Injury and Liver Regeneration after Acetaminophen Overdose. *Am. J. Pathol.* 188,  
387 1406–1418.
- 388 Camargo CA, Madden JF, Gao W, Selvan RS, Clavien PA. 1997. Interleukin-6 protects liver  
389 against warm ischemia/reperfusion injury and promotes hepatocyte proliferation in the  
390 rodent. *Hepatology.* 26, 1513–1520.
- 391 Cover C, Mansouri A, Knight TR, Bajt ML, Lemasters JJ, Pessayre D, et al. 2005. Peroxynitrite-  
392 Induced Mitochondrial and Endonuclease-Mediated Nuclear DNA Damage in  
393 Acetaminophen Hepatotoxicity. *J. Pharmacol. Exp. Ther.* 315, 879–887.
- 394 Clemens MM, Kennon-McGill S, Apte U, James LP, Finck BN, McGill MR. 2019. The inhibitor

- 395 of glycerol 3-phosphate acyltransferase FSG67 blunts liver regeneration after  
396 acetaminophen overdose by altering GSK3 $\beta$  and Wnt/ $\beta$ -catenin signaling. *Food Chem.*  
397 *Toxicol.* 125, 279–288.
- 398 Clemens MM, McGill MR, Apte U. 2019. Mechanisms and biomarkers of liver regeneration  
399 after drug-induced liver injury, in: Enna S. (Ed.), *Advances in Pharmacology*. Academic  
400 Press Inc., Cambridge, Massachusetts, pp. 241–262.
- 401 Cressman DE, Greenbaum LE, DeAngelis RA, Ciliberto G, Furth EE, Poli V, et al. 1996. Liver  
402 failure and defective hepatocyte regeneration in interleukin-6- deficient mice. *Science*.  
403 274, 1379–1383.
- 404 Fang Y, Vilella-Bach M, Flanigan A, Chen J. 2001. Phosphatidic acid-mediated activation of  
405 mitogenic mTOR signaling. *Science*. 294, 1942-1945.
- 406 Foster DA. 2013. Phosphatidic acid and lipid-sensing by mTOR. *Trends Endocrinol. Metab.* 24,  
407 272-278.
- 408 Gao RY, Wang M, Liu Q, Feng D, Wen Y, Xia Y, et al. 2019. Hypoxia-Inducible Factor (HIF)-  
409 2 $\alpha$  Reprograms Liver Macrophages to Protect Against Acute Liver Injury via the  
410 Production of Interleukin-6. *Hepatology*. 71, 2105-2117.
- 411 Gujral JS, Knight TR, Farhood A, Bajt ML, Jaeschke H. 2002. Mode of cell death after  
412 acetaminophen overdose in mice: apoptosis or oncotic necrosis? *Toxicol. Sci.* 67, 322–8.
- 413 Gunawan BK, Liu ZX, Han D, Hanawa N, Gaarde WA, Kaplowitz N. 2006. c-Jun N-Terminal  
414 Kinase Plays a Major Role in Murine Acetaminophen Hepatotoxicity. *Gastroenterology*.  
415 131, 165–178.
- 416 Hanawa N, Shinohara M, Saberi B, Gaarde WA, Han D, Kaplowitz N. 2008. Role of JNK

- 417 translocation to mitochondria leading to inhibition of mitochondria bioenergetics in  
418 acetaminophen-induced liver injury. *J. Biol. Chem.* 283, 13565–13577.
- 419 Jaeschke H. 1990. Glutathione disulfide formation and oxidant stress during acetaminophen-  
420 induced hepatotoxicity in mice in vivo: the protective effect of allopurinol. *J. Pharmacol.*  
421 *Exp. Ther.* 255, 935–41.
- 422 Jaeschke H, Akakpo JY, Umbaugh DS, Ramachandran A. 2020. Novel Therapeutic Approaches  
423 Against Acetaminophen-induced Liver Injury and Acute Liver Failure. *Toxicol. Sci.* 174,  
424 159–167.
- 425 James LP, Lamps LW, McCullough S, Hinson JA. 2003. Interleukin 6 and hepatocyte  
426 regeneration in acetaminophen toxicity in the mouse. *Biochem. Biophys. Res. Commun.*  
427 309, 857–863.
- 428 Jollow DJ, Mitchell JR, Potter WZ, Davis DC, Gillette JR, Brodie BB. 1973. Acetaminophen  
429 induced hepatic necrosis. II. Role of covalent binding in vivo. *J. Pharmacol. Exp. Ther.*  
430 187, 195–202.
- 431 Kaufman DW, Kelly JP, Rosenberg L, Anderson TE, Mitchell AA. 2002. Recent patterns of  
432 medication use in the ambulatory adult population of the United States: The Slone  
433 survey. *J. Am. Med. Assoc.* 287, 337–344.
- 434 Kon K, Kim JS, Jaeschke H, Lemasters JJ. 2004. Mitochondrial permeability transition in  
435 acetaminophen-induced necrosis and apoptosis of cultured mouse hepatocytes.  
436 *Hepatology.* 40, 1170–1179.
- 437 Kooijman EE, Chupin V, de Kruijff B, Burger KNJ. 2003. Modulation of membrane curvature  
438 by phosphatidic acid and lysophosphatidic acid. *Traffic.* 4, 162-174.

- 439 Lee WM. 2008. Etiologies of acute liver failure. *Semin. Liver Dis.* 28, 142–152.
- 440 Lim HK, Choi YA, Park W, Lee T, Ryu SH, Kim SY, et al. 2003. Phosphatidic Acid Regulates  
441 Systemic Inflammatory Responses by Modulating the Akt-Mammalian Target of  
442 Rapamycin-p70 S6 Kinase 1 Pathway. *J. Biol. Chem.* 278, 45117–45127.
- 443 Lutkewitte AJ, Schweitzer GG, Kennon-McGill S, Clemens MM, James LP, Jaeschke H, et al.  
444 2018. Lipin deactivation after acetaminophen overdose causes phosphatidic acid  
445 accumulation in liver and plasma in mice and humans and enhances liver regeneration.  
446 *Food Chem. Toxicol.* 115, 273–283.
- 447 Masubuchi Y, Bourdi M, Reilly TP, Graf ML, George JW, Pohl LR. 2003. Role of interleukin-6  
448 in hepatic heat shock protein expression and protection against acetaminophen-induced  
449 liver disease. *Biochem Biophys Res Commun.* 304, 207-212.
- 450 McGill MR, Hinson JA. 2020. The development and hepatotoxicity of acetaminophen: reviewing  
451 over a century of progress. *Drug Metab Rev.* In press. [Epub ahead of print] doi:  
452 10.1080/03602532.2020.1832112.
- 453 McGill MR, Jaeschke H. 2015. A direct comparison of methods used to measure oxidized  
454 glutathione in biological samples: 2-vinylpyridine and N-ethylmaleimide. *Toxicol. Mech.*  
455 *Methods.* 25, 589–595.
- 456 McGill MR, Lebofsky M, Norris HRK, Slawson MH, Bajt ML, Xie Y, et al. 2013. Plasma and  
457 liver acetaminophen-protein adduct levels in mice after acetaminophen treatment: Dose-  
458 response, mechanisms, and clinical implications. *Toxicol. Appl. Pharmacol.* 269, 240–  
459 249.
- 460 McGill MR, Sharpe MR, Williams CD, Taha M, Curry SC, Jaeschke H. 2012. The mechanism

461 underlying acetaminophen-induced hepatotoxicity in humans and mice involves  
462 mitochondrial damage and nuclear DNA fragmentation. *J. Clin. Invest.* 122, 1574–1583.

463 McGill MR, Yan HM, Ramachandran A, Murray GJ, Rollins DE, Jaeschke H. 2011. HepaRG  
464 cells: A human model to study mechanisms of acetaminophen hepatotoxicity.  
465 *Hepatology.* 53, 974–982.

466 Mitchell JR, Jollow DJ, Potter WZ, Gillette JR, Brodie BB. 1973. Acetaminophen induced  
467 hepatic necrosis. IV. Protective role of glutathione. *J. Pharmacol. Exp. Ther.* 187, 211–  
468 217.

469 Muldrew KL, James LP, Coop L, McCullough SS, Hendrickson HP, Hinson JA, et al. 2002.  
470 Determination of acetaminophen-protein adducts in mouse liver and serum and human  
471 serum after hepatotoxic doses of acetaminophen using high-performance liquid  
472 chromatography with electrochemical detection. *Drug Metab. Dispos.* 30, 446–451.

473 Mullins ME, Yeager LH, Freeman WE. 2020. Metabolic and mitochondrial treatments for severe  
474 paracetamol poisoning: a systematic review. *Clin Toxicol.* In press. [Epub ahead of print]  
475 doi: 10.1080/15563650.2020.1798979.

476 Nakagawa H, Maeda S, Hikiba Y, Ohmae T, Shibata W, Yanai A, et al. 2008. Deletion of  
477 Apoptosis Signal-Regulating Kinase 1 Attenuates Acetaminophen-Induced Liver Injury  
478 by Inhibiting c-Jun N-Terminal Kinase Activation. *Gastroenterology.* 135, 1311–1321.

479 Pokotylo I, Kravets V, Martinec J, Ruelland E. 2018. The phosphatidic acid paradox: Too many  
480 actions for one molecule class? Lessons from plants. *Prog. Lipid Res.* 71, 43-53.

481 Purpura M, Jäger R, Joy JM, Lowery RP, Moore JD, Wilson JM. 2013. Effect of oral  
482 administration of soy-derived phosphatidic acid on concentrations of phosphatidic acid

- 483 and lyso-phosphatidic acid molecular species in human plasma. *J. Int. Soc. Sports Nutr.*  
484 2013, P22.
- 485 Ramachandran A, McGill MR, Xie Y, Ni HM, Ding WX, Jaeschke H. 2013. Receptor interacting  
486 protein kinase 3 is a critical early mediator of acetaminophen-induced hepatocyte  
487 necrosis in mice. *Hepatology.* 58, 2099–2108.
- 488 Reid AB, Kurten RC, McCullough SS, Brock RW, Hinson JA. 2005. Mechanisms of  
489 acetaminophen-induced hepatotoxicity: Role of oxidative stress and mitochondrial  
490 permeability transition in freshly isolated mouse hepatocytes. *J. Pharmacol. Exp. Ther.*  
491 312, 509–516.
- 492 Río A, Gassull MA, Aldeguer X, Ojanguren I, Cabré E, Fernández E. 2008. Reduced liver injury  
493 in the interleukin-6 knockout mice by chronic carbon tetrachloride administration. *Eur. J.*  
494 *Clin. Invest.* 38, 306–316.
- 495 Selzner M, Camargo CA, Clavien PA. 1999. Ischemia impairs liver regeneration after major  
496 tissue loss in rodents: Protective effects of interleukin-6. *Hepatology.* 30, 469–475.
- 497 Shad BJ, Smeuninx B, Atherton PJ, Breen L. 2015. The mechanistic and ergogenic effects of  
498 phosphatidic acid in skeletal muscle. *Appl. Physiol. Nutr. Metab.* 40, 1233–1241.
- 499 Shinohara M, Ybanez MD, Win S, Than TA, Jain S, Gaarde WA, et al. 2010. Silencing glycogen  
500 synthase kinase-3 $\beta$  inhibits acetaminophen hepatotoxicity and attenuates JNK activation  
501 and loss of glutamate cysteine ligase and myeloid cell leukemia sequence. *J. Biol. Chem.*  
502 285, 8244–8255.
- 503 Tolson JK, Dix DJ, Voellmy RW, Roberts SM. 2006. Increased hepatotoxicity of acetaminophen  
504 in Hsp70i knockout mice. *Toxicol. Appl. Pharmacol.* 210, 157-162.

505 Win S, Than TA, Min RWM, Aghajan M, Kaplowitz N. 2016. c-Jun N-terminal kinase mediates  
506 mouse liver injury through a novel Sab (SH3BP5)-dependent pathway leading to  
507 inactivation of intramitochondrial Src. *Hepatology*. 63, 1987–2003.  
508



509 **Figure Legends**

510 **Figure 1. Post-treatment with exogenous PA protects against early APAP hepatotoxicity.**

511 Mice were treated with 250 mg/kg APAP at 0 h, followed by vehicle (Veh) or PA at 2 h. Blood  
512 and liver tissue were collected at 6 h. (A) Serum ALT activity. (B) H&E-stained liver sections.  
513 Data expressed as mean  $\pm$  SE for n = 10 per group. \*p<0.05 vs. APAP plus Veh.

514 **Figure 2. Post-treatment with exogenous PA does not affect canonical mechanisms of**

515 **APAP hepatotoxicity.** Mice were treated with 250 mg/kg APAP at 0 h, followed by vehicle  
516 (Veh) or PA at 2 h. Liver tissue was collected at 6 h. (A) Total glutathione (GSH+GSSG) in  
517 liver. (B) APAP-protein adducts in liver. (C) Absolute oxidized glutathione (GSSG) in liver. (D)  
518 GSSG as the percentage of total glutathione (%GSSG). (E) Immunoblots for total and  
519 phosphorylated JNK. (F) JNK densitometry. (G) Immunoblots for AIF, cytochrome c, and  $\beta$ -  
520 actin. (H) Immunoblots for total and phosphorylated (Ser9) GSK3 $\beta$ . (I) Oil Red O staining in  
521 liver sections. Data expressed as mean  $\pm$  SE for n = 5 per group. No statistically significant  
522 differences were detected.

523 **Figure 3. Post-treatment with exogenous PA activates IL-6 signaling in the liver.** Mice were

524 treated with 250 mg/kg APAP or vehicle alone at 0 h, followed by vehicle (Veh) or PA at 2 h.  
525 Blood and liver tissue were collected at 6 h. (A) Gene ontology (Biological Process) analysis of  
526 vehicle alone vs. APAP+vehicle. (B) Hierarchical clustering of genes in the APAP+vehicle and  
527 APAP+PA groups. (C) Serum IL-6 values. Data expressed as mean  $\pm$  SE for n = 5 per group.  
528 \*p<0.05 vs. APAP plus Veh.

529 **Figure 4. Post-treatment with exogenous PA does not protect in IL-6 KO mice.** WT and IL-6

530 KO mice were treated with 350 mg/kg APAP at 0 h, followed by vehicle or PA at 2 h. Blood and

531 liver tissue were collected at 6 h. (A) Serum ALT activity in WT mice. (B) Serum ALT activity  
532 in KO mice. (C) H&E-stained liver sections from both genotypes. Data expressed as mean  $\pm$  SE  
533 for n = 5-6 per group. \*p<0.05 vs. APAP plus Veh.

534 **Figure 5. Exogenous PA induces hepatic Hsp70 in WT but not IL-6 KO mice.**

535 Immunoblotting was performed in liver lysates from the WT and KO mice. (A) Hsp70 and total  
536 protein loading in liver tissue from WT mice. (B) Hsp70 and total protein loading in liver tissue  
537 from IL-6 KO mice. (C,D) Densitometry. Data expressed as mean  $\pm$  SE for n = 5-6 per group.  
538 \*p<0.05 vs. APAP plus Veh.

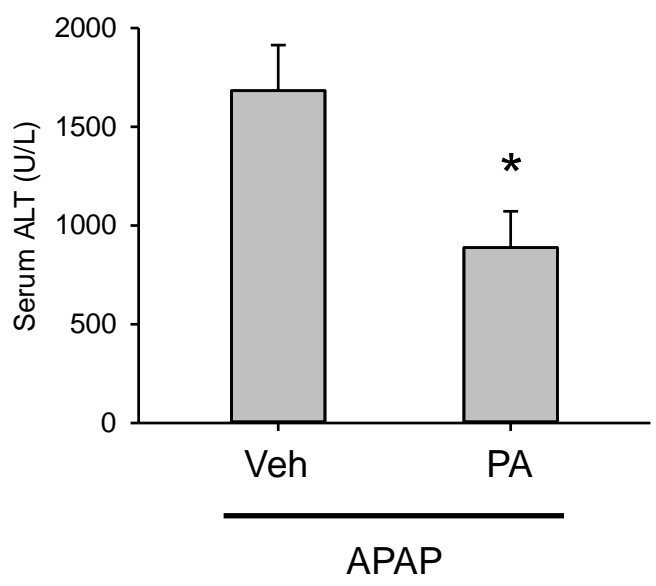
539 **Figure 6. The source of IL-6 is extrahepatic and likely includes white adipose tissue.** In one  
540 experiment, mice were treated with 250 mg/kg APAP at 0 h, followed by vehicle (Veh) or PA at  
541 2 h. Where indicated, mice were pre-treated for 24 h with liposomal clodronate (LC). Blood and  
542 liver tissue were collected at 6 h. In a second experiment, mice were treated with 20 m/kg PA or  
543 vehicle and various tissues were collected 4 h later. (A) Liver IL-6 mRNA from the first  
544 experiments. (B) Serum ALT activity from the first experiment. (C) F4/80  
545 immunohistochemistry in liver tissue sections from the first experiment. (D) IL-6 mRNA from  
546 the second experiment. Data expressed as mean  $\pm$  SE for n = 5-10 per group. \*p<0.05 vs. APAP  
547 plus Veh.

548 **Figure 7. Late post-treatment with exogenous PA does not affect liver regeneration.** Mice

549 were treated with 250 mg/kg APAP at 0 h, followed by vehicle (Veh) or PA at 6, 24, and 48 h.  
550 Blood and liver tissue were collected at 24 and 52 h. (A) Serum ALT. (B) H&E-stained liver  
551 sections. (C) Immunoblot for proliferating cell nuclear antigen (Pcna) and  $\beta$ -actin. Data  
552 expressed as mean  $\pm$  SE for n = 4-5 per group. \*p<0.05 vs. APAP plus Veh.

Figure 1.

A



B

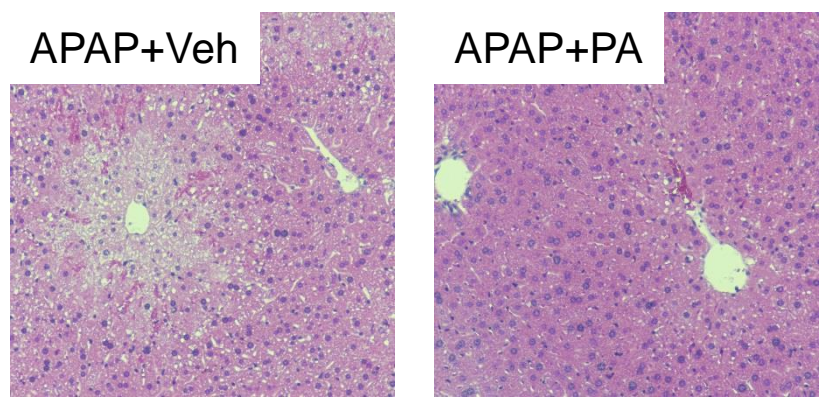


Figure 2.

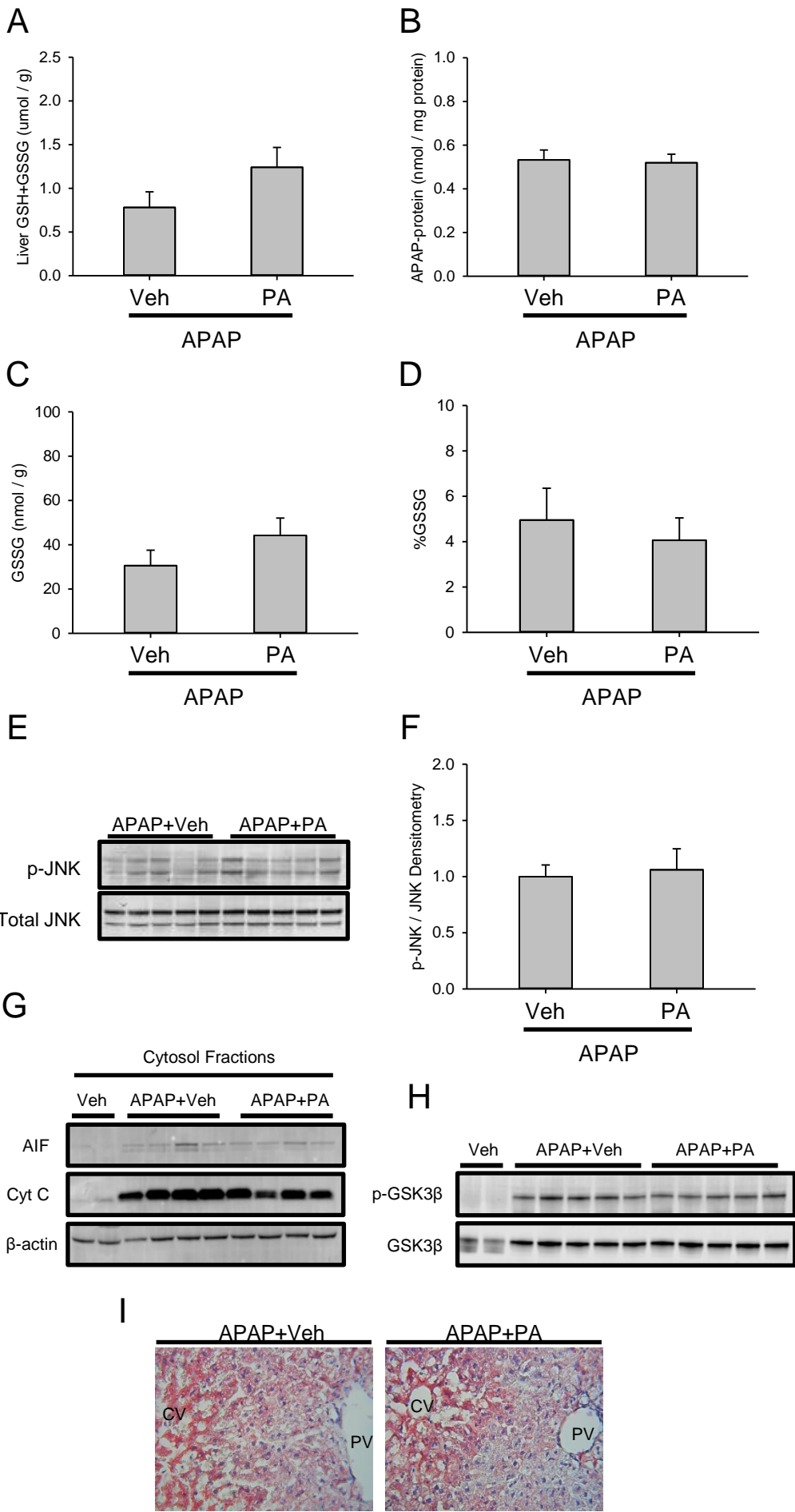
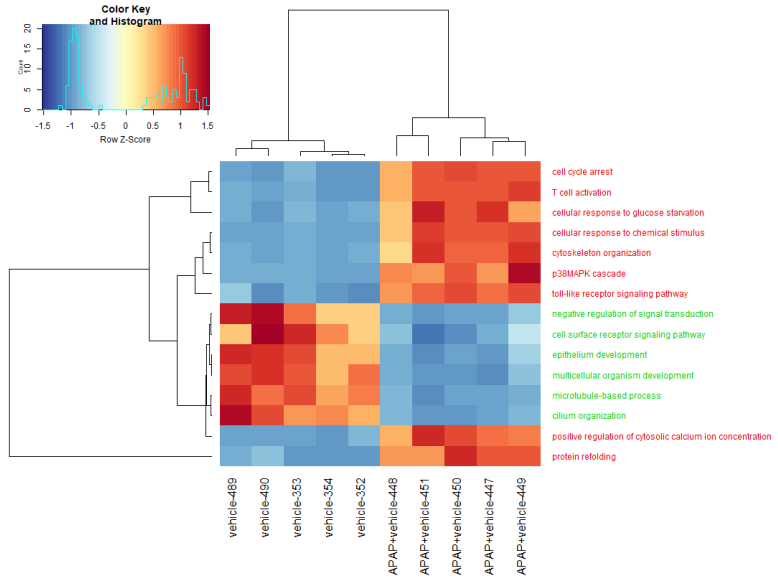
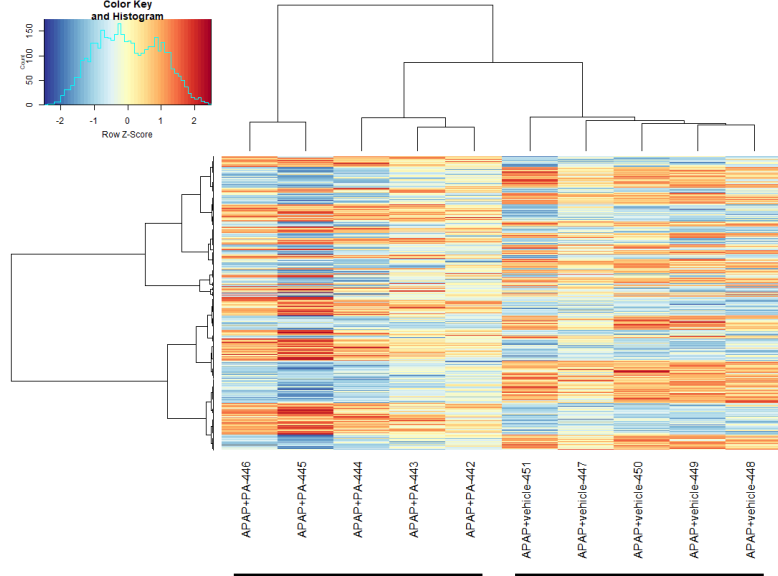


Figure 3.

A



B



C

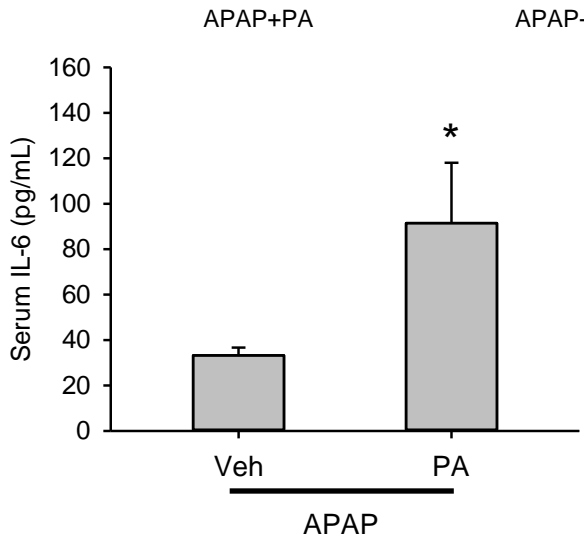


Figure 4.

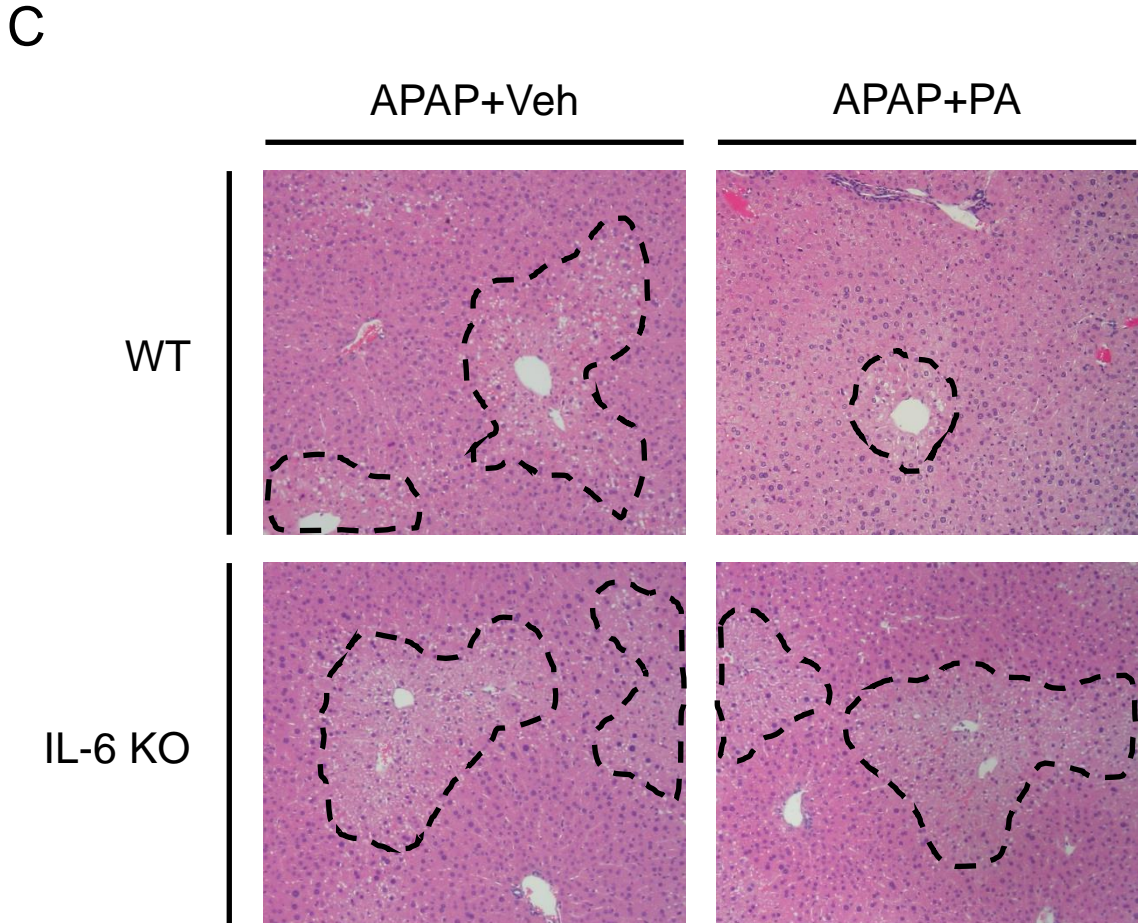
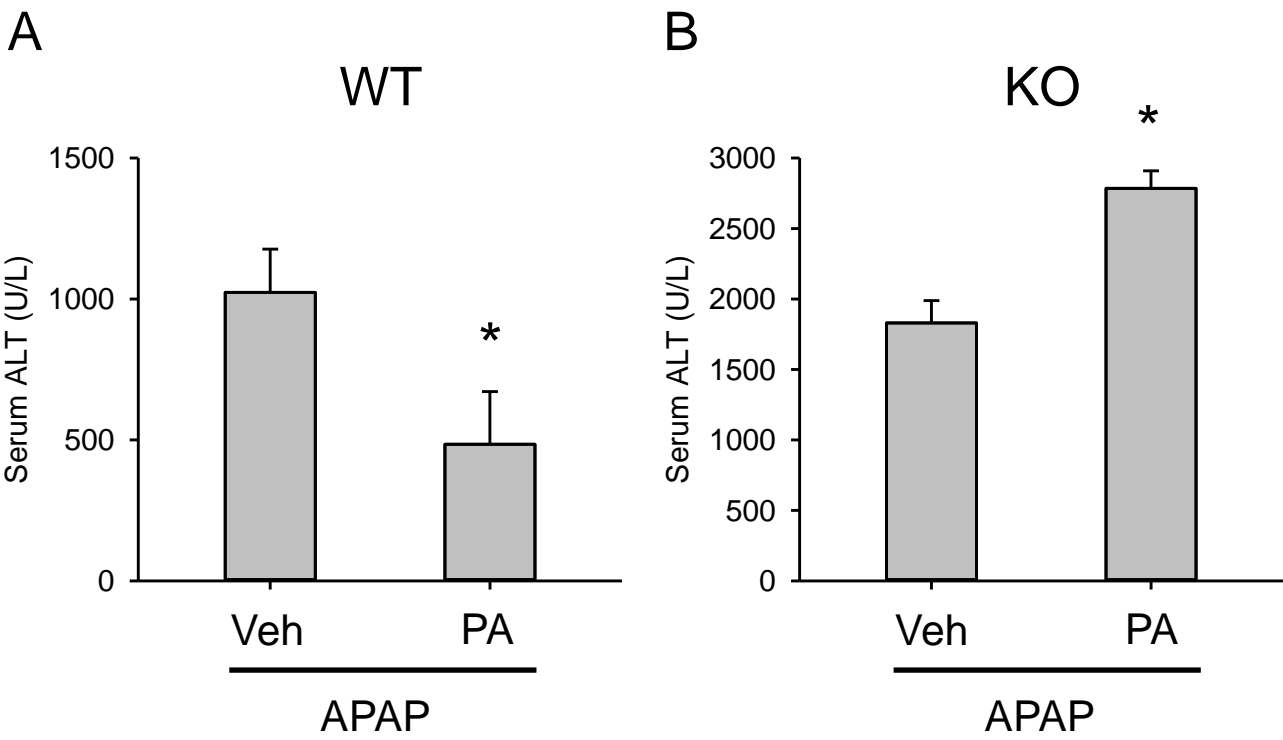


Figure 5.

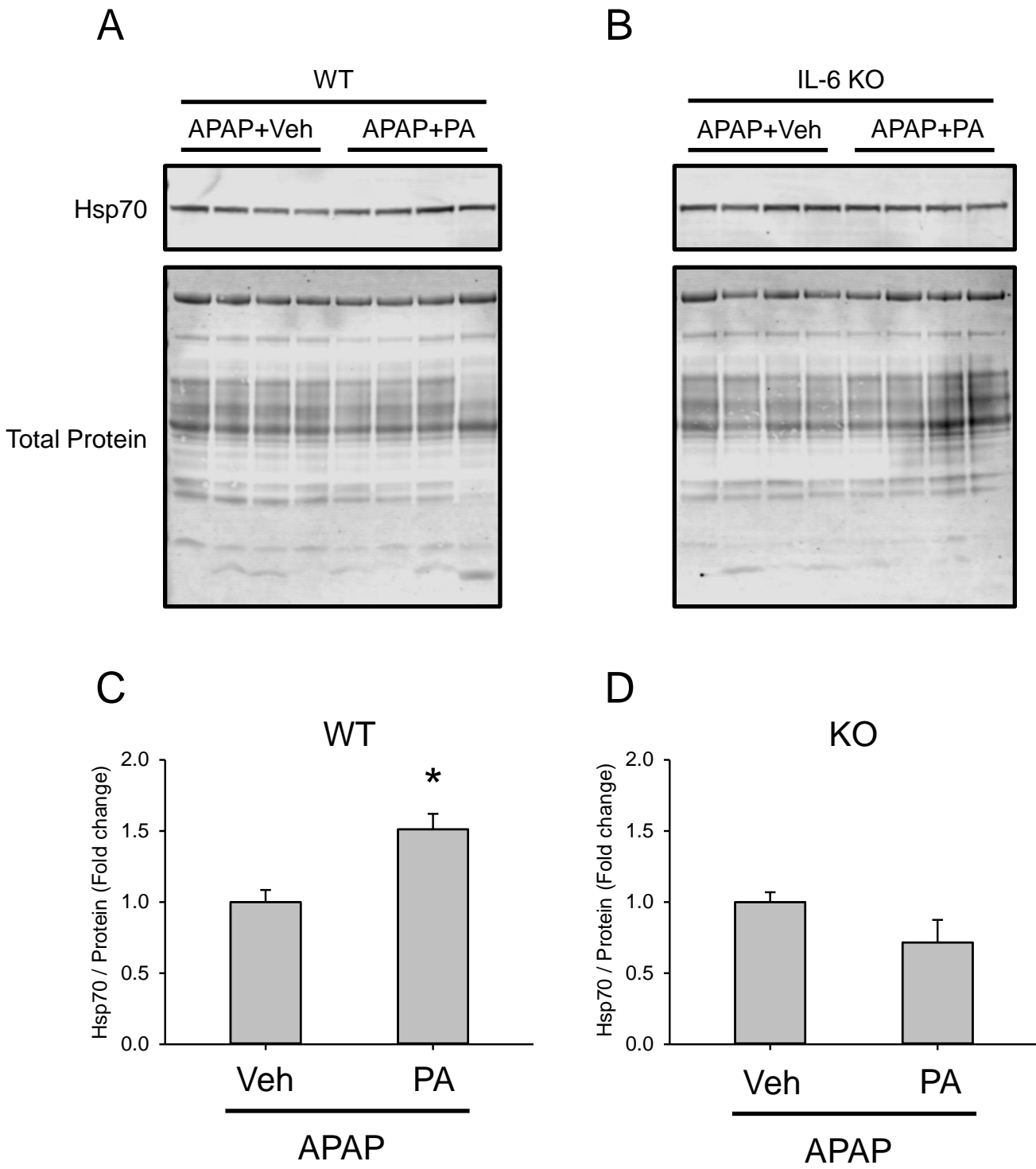


Figure 6.

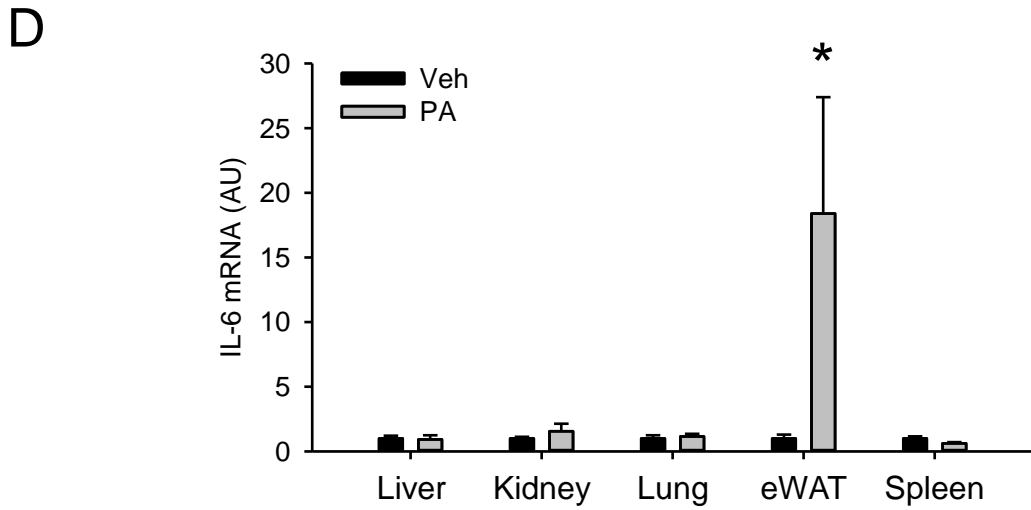
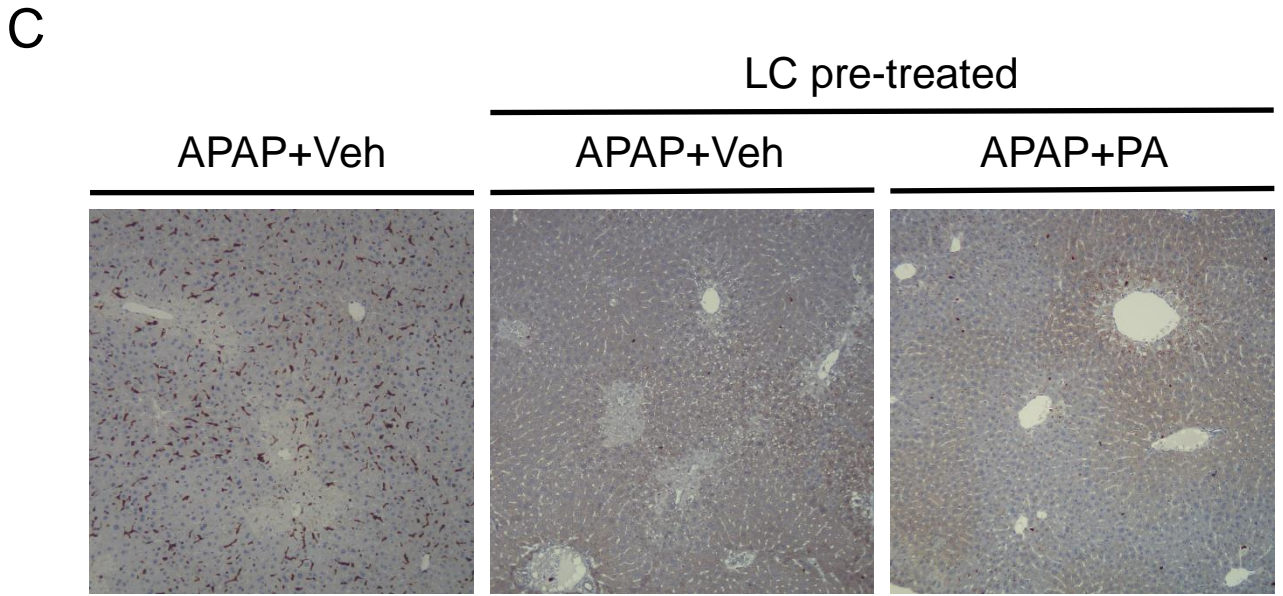
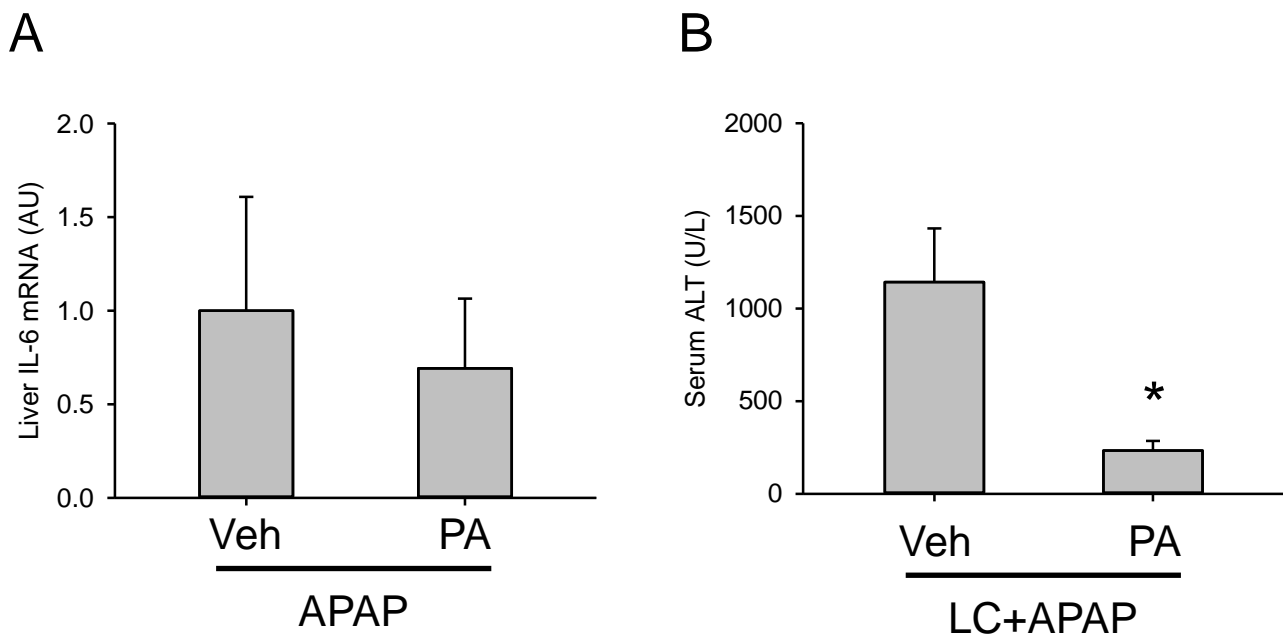
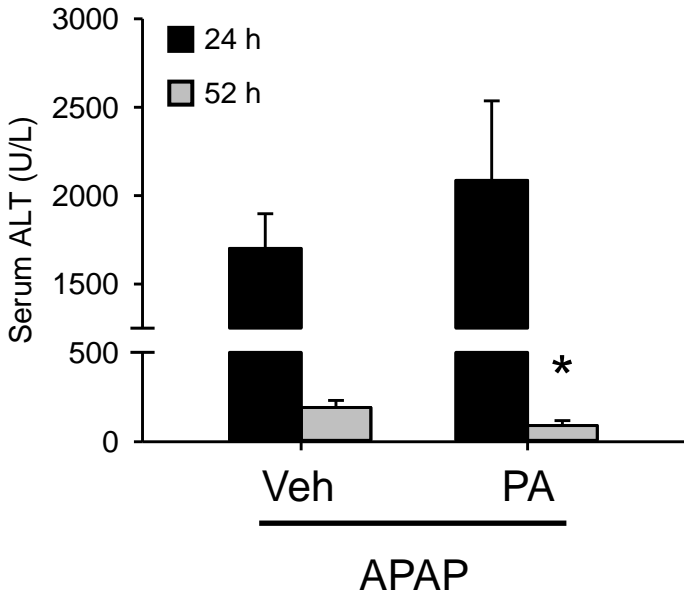


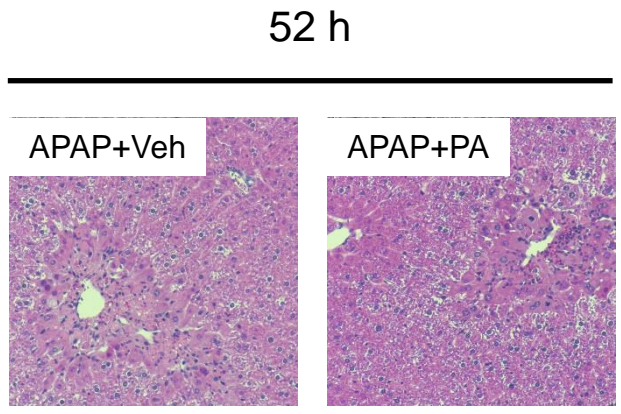


Figure 7.

A



B



C

